Injection locking of the gyrotropic vortex motion in a nanopillar

R. Lehndorff, D. E. Bürgler, C. M. Schneider, and Z. Celinski

Injection locking of the gyrotropic vortex motion in a nanopillar

R. Lehndorff,[1] D. E. Bürgler,[1,a)] C. M. Schneider,[1] and Z. Celinski[2]

[1]*Institute of Solid State Research, Electronic Properties (IFF-9) and JARA-FIT, Research Center Jülich GmbH, D-52425 Jülich, Germany*
[2]*Center for Magnetism and Magnetic Nanostructures, University of Colorado at Colorado Springs, Colorado 80918, USA*

Spin-torque oscillators (STOs) are a promising application for the spin-transfer torque effect. The major challenge lies in pushing the STO's microwave output power to useful levels, e.g., by operating an array of STOs in a synchronized, phase-locked mode. Our experiment on metallic, giant magnetoresistance-type nanopillars focuses on the influence of external high-frequency signals on the current-driven vortex dynamics and demonstrates the injection locking of the gyrotropic mode. We find a gap of about three orders of magnitude between the high-frequency power emitted by one oscillator and the power needed for phase-locking. © *2010 American Institute of Physics*. [doi:10.1063/1.3498009]

The action of spin-polarized currents onto a magnetic system—the spin-transfer torque—offers a novel handle on magnetization dynamics. One of the potential applications is seen in the so-called spin-torque oscillators (STOs). These are pillar-shaped structures with a "fixed" magnetic layer acting as a polarizer for the electric current and a second "free" magnetic layer the magnetization of which oscillates under the impact of the spin-polarized current. The magnetoresistive response due to giant or tunneling magnetoresistance (GMR, TMR) in the magnetic layered structure turns the nanometer-scaled STO structures into sources for high-frequency (HF) signals in the gigahertz range. The frequency is tunable via the direct current (dc) and the external magnetic field. However, the HF output power of an STO is presently far too low for applications. This is particularly true for metallic, GMR-based STOs due to their low MR ratio of only a few percent yielding output powers in the picowatt to low nanowatt regime. TMR-based STOs with TMR ratios of the order of 100% have been shown to generate about 1 μW of output power.[1]

Ongoing research aims at strategies to significantly increase the output power. To advance on this, each STO should emit the maximum achievable power. We have recently pointed out a way to maximize the power by operating an STO in the vortex mode, i.e., by exciting with dc current the gyrotropic vortex mode instead of the precessional modes of the quasiuniform, single-domain state.[2] A further advantage of vortex STOs is that they intrinsically operate in zero external field. This can also be achieved in single-domain STOs, however, only when using carefully selected layer structures or geometries,[3–5] which impose design restrictions.

Generally, the excitation of an array of STOs in a synchronized, phase-locked manner is believed to deliver a significant power increase, as N coherently coupled STOs emit up to the N^2-fold power. The STO–STO coupling can be achieved in two ways. First, by spin waves in a common ferromagnetic layer, as has been already demonstrated for two[6–8] and four[9] STOs. Due to the fast decay of spin waves this interaction is short-range and requires a STO–STO sepa-

ration of the order of the STO's diameter, i.e., clearly below 1 μm. The second coupling mechanism via microwaves propagating in common electrodes[10,11] permits a larger STO separation because electrical microwave signals propagate with negligible losses over long distances. Experimentally, this situation has been addressed by injection locking experiments, which study the interaction of a STO with an externally applied HF signal in order to investigate conditions for synchronization and phase-locking. Rippard *et al.*[12] have shown the injection locking of a single-domain STO.

In this letter, we demonstrate phase-locking of the dc current-driven gyrotropic vortex motion in a vortex STO to external HF signals, and derive from the HF amplitude dependence of the locking criteria for the required STO output power for synchronization.

We fabricate our samples from epitaxial (001)-oriented multilayers of Ag 150 nm/Fe 2 nm/Ag 6 nm/Fe 20 nm/Au 50 nm grown by molecular beam epitaxy.[13] Cylindrical pillars of 230 nm diameter are fabricated by means of optical and electron beam lithography combined with ion beam etching, reactive ion etching, and lift-off.[13] The upper 20 nm thick Fe layer and the Au 50 nm cap layer form the pillar while the remaining layers Ag 150 nm/Fe 2 nm/Ag 6 nm constitute the 15 μm wide bottom electrode [inset of Fig. 1(a)]. The electrode layout allows for contacting by two microwave probes via coplanar waveguides. One is used to inject a dc current and an HF current (f_{ext}) from a network analyzer. The two currents are combined in a bias-T. The second probe is connected to a 30 dB amplifier and a spectrum analyzer (see top of Fig. 2). The experiments were conducted at 300 K in a microwave probe station with an in-plane magnetic field of up to 300 mT.

In Fig. 1(a) we compare measurements of the MR in current-perpendicular-plane (CPP) geometry in an in-plane magnetic field (CPP-GMR) with corresponding micromagnetic simulations. The nanodisk has two static magnetic states. The quasiuniform onion state occurs when the field is reduced after saturation and the vortex state nucleates at low fields after field reversal. The magnetization of the extended layer is saturated along an easy axis for fields larger than 20 mT. From this we can identify the magnetization states of the Fe layers at various fields.[2] On this basis we know how to

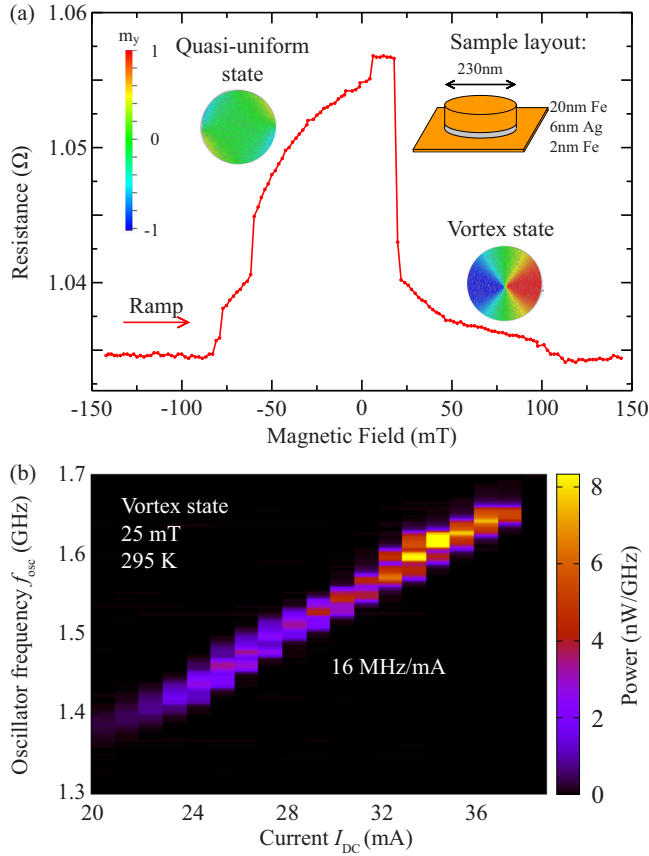a)Electronic mail: d.buergler@fz-juelich.de.

FIG. 1. (Color online) (a) CPP-GMR in comparison with micromagnetic calculations of the magnetization structure in the nanodisk (inset: sample layout). (b) Power spectra of the current-induced gyrotropic mode as a function of dc current I_{dc}.
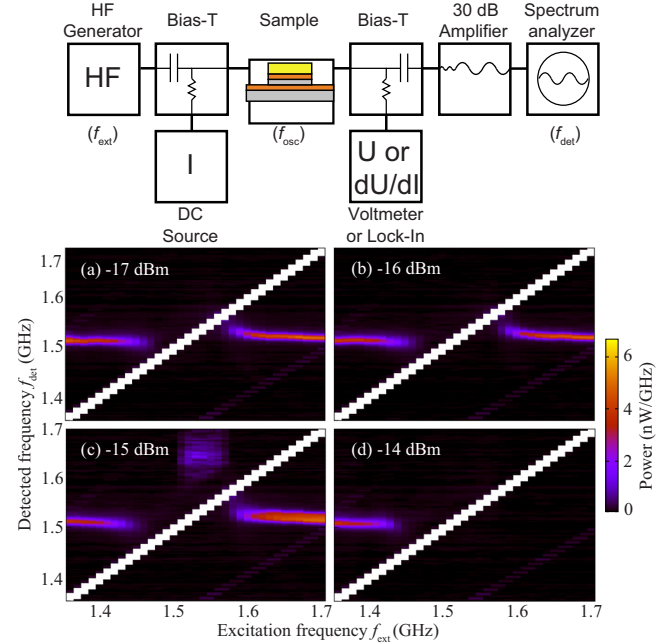

FIG. 2. (Color online) Measurement setup for injection locking and power spectra (f_{det}, vertical axis) of the current-induced gyrotropic mode as a function of HF excitation frequency (f_{ext}, horizontal axis) measured for different excitation amplitudes as indicated. The intensity at f_{ext} exceeds the color scale and appears as diagonal white lines.

prepare a vortex state in the nanodisk while, at the same time, the magnetization of the extended layer is saturated along a magnetic easy axis of bcc Fe, e.g., by applying +25 mT after negative saturation.

Applying positive dc currents (i.e., electron flow from the nanomagnet to the extended layer) in the range of 20 to 39 mA the vortex state is excited by spin-transfer torque into the gyrotropic mode[14] that shows up as an HF voltage signal derived from the GMR [Fig. 1(b)]. Its frequency f_{osc} increases linearly with the current at a rate of 16 MHz/mA.[2] These findings are in agreement with a mechanism for spin-transfer induced gyrotropic motion of a vortex in a spin-valve nanostructure with an in-plane magnetized polarizer proposed by Khvalkovskiy *et al.*[15] The model assumes a nonuniform, i.e., symmetry-breaking magnetization of the polarizer. An alternative mechanism may be related to the strong angular asymmetry of the spin-transfer torque in Fe/Ag/Fe(001) structures,[16] which also breaks the symmetry in the sample plane.[17]

Adding a HF component to the driving current we are able to demonstrate phase-locking of the dc current-induced gyrotropic motion to electric HF signals even if they are slightly out of tune. Figure 2(a) shows a measurement, where the vortex was excited by a current of 32 mA to a frequency of $f_{osc}=1.518$ GHz while an external signal of −17 dB m or 20 μW was swept from $f_{ext}=1.35$ to 1.7 GHz. This leads to a clear shift in the vortex frequency between 1.42 and 1.61 GHz. From 1.46 to 1.57 GHz the vortex frequency f_{osc} is completely locked to the external signal f_{ext} and is thus masked by it. Upon an amplitude increase [Fig. 2(b)] the

phase-locking ranges widen without qualitative changes. At −15 dB m [Fig. 2(c)] an additional signal of 1.65 GHz shows up in the right-hand part of the phase-locked regime and the signal shape and intensity changes for external frequencies f_{ext} above 1.6 GHz. The origin of these features is not clear. Micromagnetic simulations are required to relate them to modifications of the gyrotropic mode, e.g., periodic vortex core reversals,[15] or the presence of additional excited modes at increased HF amplitude. Finally, for strongest excitations at −14 dB m [Fig. 2(d)] the vortex signal is lost above 1.5 GHz when sweeping through the locking regime from low to high f_{ext}. The dc resistance after completing the frequency sweep is larger than before, which—based on Fig. 1—must be identified with the quasiuniform magnetization state. Thus, the vortex has been expelled from the sample while being phase-locked to the HF signal. This may happen, when the radius of the gyrotropic trajectory strongly increases due to the excitation and the vortex finally hits the boundary of the nanodisk.

In order to evaluate the synchronization behavior in-depth we fit the frequency variation f_{osc} in the forced vortex motion with the frequency f_{ext} of the injected HF signal to a formula derived by Slavin and Tiberkevich for nonlinear oscillators as follows [Eq. (48b) of Ref. 18]:

$$f_{osc} = f_{ext} + \text{sign}(f_0 - f_{ext})\sqrt{(f_0 - f_{ext})^2 - \Delta^2}, \quad (1)$$

where $f_0 = f_{osc}(I_{HF}=0)$ is the frequency of the free-running vortex STO and Δ is the phase-locking range. An example of a fit is shown in the inset of Fig. 3. The main figure shows an increase in Δ with increasing amplitude of the external signal in accordance with the linear dependence predicted by Slavin and Tiberkevich.[18] The conversion from HF power to HF current amplitudes I_{HF} is given by the impedance of the sample (11 Ω at 1.5 GHz) that we have measured with a network analyzer. However, the linear extrapolation to zero excitation amplitude (dashed line in Fig. 3) yields a nonva-
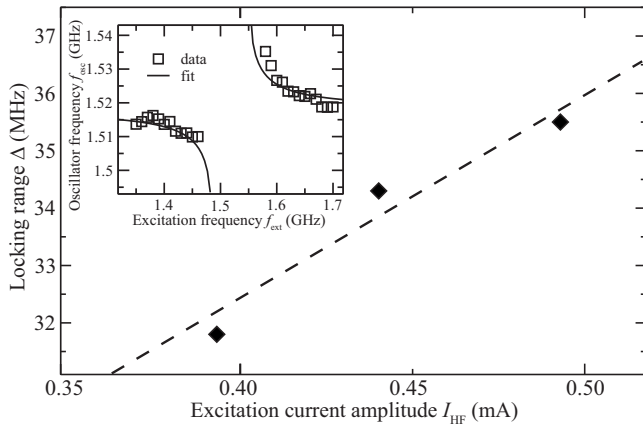
FIG. 3. Locking range Δ as a function of the external HF excitation amplitude. The dashed line is a linear fit. Inset: Fit (solid line) of Eq. (1) to the experimental locking behavior for $I_{dc}=32$ mA and -16 dB m.

nishing locking range of about 18 MHz. This inconsistency may be due to the fact that the theoretical model assumes only a weak excitation. Our data indicates that the widening of the locking range Δ with the excitation amplitude proceeds slower for strong excitation.

Figure 4 shows the locking behavior of the vortex STO when excited by a fixed dc current of 32 mA and an external 1.55 GHz signal of variable amplitude. For weak excitation the STO is not influenced by the HF signal and emits at its free-running frequency $f_0 \approx 1.52$ GHz. With increasing HF amplitude the STO tends to adjust to the external frequency and phase-locks for excitation amplitudes exceeding -18 dB m. The locking process is accompanied by a weakening and broadening of the STO signal. The HF signal generated by the magnetization dynamics in the pillar and the externally applied HF signal passing through the pillar are reaching the spectrum analyzer via a common pathway (right-hand branch of the setup in Fig. 2). Therefore, we can directly determine the ratio between the power required for phase-locking and the power generated by the pillar from the measured spectra and obtain a ratio of about 3300. The HF signal is attenuated in cables, connectors, the waveguides on the sample, and due to impedance mismatch, e.g., between leads and pillar. We characterize the sum of all these effects by measuring the transmission from the HF generator to the spectrum analyzer. Based on this transmission value and the symmetry of the setup we estimate the external HF power at -18 dB m reaching the pillar to be of the order of 1.3 μW. Thus, the vortex STO generates roughly 0.4 nW of microwave power. This low value is related to the low absolute

resistance and low GMR ratio, which result in small resistance changes due to the magnetization dynamics. We emphasize that the physics of the vortex dynamics described in this letter is not affected by the weak conversion to output power.

Consequently, the output power of our GMR-based vortex STO is about three orders of magnitude too small to phase-lock another vortex STO. Under these conditions synchronization of an array of vortex STOs seems unlikely, unless the output power of each single STO is significantly increased, e.g., by employing highly spin-polarized ferromagnetic electrode materials (Heusler alloys[19]) or TMR-based structures with much higher MR ratios.

In conclusion, we demonstrated the possibility to phase-lock the current-driven vortex motion in an STO to an external HF signal, being a prerequisite for the synchronization of vortex STOs. The relative locking range $2\Delta/f_0 \approx 5\%$ is rather large and allows for a distribution of free-running frequencies in a STO array, which seems to be compatible with present fabrication technology. The power requirements for synchronization, however, call for STOs with much higher output power and for optimization of the synchronization efficiency, e.g., by appropriate phase control.[20]

[1] A. M. Deac, A. Fukushima, H. Kubota, H. Maehara, Y. Suzuki, S. Yuasa, Y. Nagamine, K. Tsunekawa, D. D. Djayaprawira, and N. Watanabe, Nat. Phys. **4**, 803 (2008).
[2] R. Lehndorff, D. E. Bürgler, S. Gliga, R. Hertel, P. Grünberg, and C. M. Schneider, Phys. Rev. B **80**, 054412 (2009).
[3] O. Boulle, V. Cros, J. Grollier, L. G. Pereira, C. Deranlot, F. Petroff, G. Faini, J. Barnas, and A. Fert, Nat. Phys. **3**, 492 (2007).
[4] T. Devolder, A. Meftah, K. Ito, J. A. Katine, P. Crozat, and C. Chappert, J. Appl. Phys. **101**, 063916 (2007).
[5] R. Lehndorff, D. E. Bürgler, A. Kakay, R. Hertel, and C. M. Schneider, IEEE Trans. Magn. **44**, 1951 (2008).
[6] S. Kaka, M. Pufall, W. H. Rippard, T. J. Silva, S. E. Russek, and J. Katine, Nature (London) **437**, 389 (2005).
[7] F. B. Mancoff, N. D. Rizzo, B. N. Engel, and S. Tehrani, Nature (London) **437**, 393 (2005).
[8] M. R. Pufall, W. H. Rippard, S. E. Russek, S. Kaka, and J. A. Katine, Phys. Rev. Lett. **97**, 087206 (2006).
[9] A. Ruotolo, V. Cros, B. Georges, A. Dussaux, J. Grollier, C. Deranlot, R. Guillemet, K. Bouzehouane, S. Fusil, and A. Fert, Nat. Nanotechnol. **4**, 528 (2009).
[10] J. Grollier, V. Cros, and A. Fert, Phys. Rev. B **73**, 060409 (2006).
[11] B. Georges, J. Grollier, M. Darques, V. Cros, C. Deranlot, B. Marcilhac, G. Faini, and A. Fert, Phys. Rev. Lett. **101**, 017201 (2008).
[12] W. H. Rippard, M. R. Pufall, S. Kaka, T. J. Silva, S. E. Russek, and J. A. Katine, Phys. Rev. Lett. **95**, 067203 (2005).
[13] H. Dassow, R. Lehndorff, D. E. Bürgler, M. Buchmeier, P. A. Grünberg, C. M. Schneider, and A. van der Hart, Appl. Phys. Lett. **89**, 222511 (2006).
[14] K. Y. Guslienko, B. A. Ivanov, V. Novosad, Y. Otani, H. Shima, and K. Fukamichi, J. Appl. Phys. **91**, 8037 (2002).
[15] A. V. Khvalkovskiy, J. Grollier, N. Locatelli, Y. V. Gorbunov, K. A. Zvezdin, and V. Cros, Appl. Phys. Lett. **96**, 212507 (2010).
[16] R. Lehndorff, D. E. Bürgler, A. Kakay, R. Hertel, and C. M. Schneider, Phys. Rev. B **76**, 214420 (2007).
[17] V. Sluka and D. E. Bürgler (unpublished).
[18] A. Slavin and V. Tiberkevich, IEEE Trans. Magn. **45**, 1875 (2009).
[19] T. Iwase, Y. Sakuraba, S. Bosu, K. Saito, S. Mitani, and K. Takanashi, Appl. Phys. Express **2**, 063003 (2009).
[20] Y. Zhou, J. Persson, S. Bonetti, and J. Åkerman, Appl. Phys. Lett. **92**, 092505 (2008).
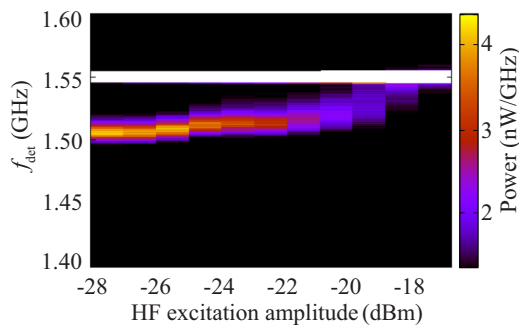

FIG. 4. (Color online) Locking behavior of a vortex STO as a function of the HF excitation amplitude at $f_{ext}=1.55$ GHz and $I_{dc}=32$ mA. Locking occurs at about -18 dB m.